

# 1 Impact of division rate and cell size on gene expression 2 noise

3 François Bertaux<sup>1,2,3</sup>, Samuel Marguerat<sup>2,3,4</sup>, Vahid Shahrezaei<sup>1,4</sup>

4 1. Department of Mathematics, Imperial College London, London SW7 2AZ, UK

5 2. MRC London Institute of Medical Sciences (LMS), London W12 0NN, UK

6 3. Institute of Clinical Sciences (ICS), Faculty of Medicine, Imperial College London,  
7 London, W12 0NN, UK

8 4. To whom correspondence should be addressed

## 9 Abstract

10 Cells physiology adapts globally to changes in growth conditions. This includes changes in  
11 cell division rate, cell size, and gene expression. These global physiological changes are  
12 expected to affect noise in gene expression in addition to average molecule concentrations.  
13 Gene expression is inherently stochastic, and the amount of noise in protein levels depends  
14 on both gene expression rates and the cell division cycle.

15 Here, we model stochastic gene expression inside growing and dividing cells to study the  
16 effect of cell division rate on noise in gene expression. We use a modelling framework and  
17 parameters relevant to *E. coli*, for which abundant quantitative data is available.

18 We find that coupling of transcription rate (but not translation rate) with the division  
19 rate results in homeostasis of both protein concentration and noise across conditions.  
20 Interestingly, we find that the increased cell size at fast division rates, observed in *E. coli*  
21 and other unicellular organisms, prevents noise increase even for proteins with decreased  
22 average expression at faster growth.

23 We then investigate the functional importance of these regulations by considering gene

24 regulatory networks that exhibit bistability and oscillations. We find that the topology of  
25 the gene regulatory network can affect its robustness with respect to changes in division  
26 rate in complex and unexpected ways. In particular, a simple model of persistence based  
27 on global physiological feedback predicts an increase in the persistence population at low  
28 division rates.

29 Our study reveals a potential role for cell size regulation in the global control of gene  
30 expression noise. It also highlights that understanding of circuits' robustness across growth  
31 conditions is key for the effective design of synthetic biological systems.

32 **Keywords** stochastic gene expression, growth rate, division rate, bistable switches, circa-  
33 dian oscillations, *E. coli*

## 34 **Introduction**

35 Microbial species can proliferate in a variety of environmental conditions. How genomes  
36 achieve this phenotypic flexibility is a fundamental biological question. Regulated gene  
37 expression is a key mechanism by which cells adapt physiologically to changing environ-  
38 ments. For example, different types of metabolic enzymes are expressed to support growth  
39 on different carbon sources (Görke & Stülke, 2008). Despite this remarkable adaptability,  
40 the rate at which cells proliferate can vary strongly from one environment to another. For  
41 example, *E. coli* division rates range between 0.5 to 3.5 doublings per hour in response to  
42 different carbon sources (Taheri-Araghi *et al*, 2015).

43 In addition to specific gene regulation, changes in division rate are accompanied by global  
44 physiological changes (Figure 1), such as changes in cell size at division and gene expression.  
45 Global changes in gene expression with cellular growth rates are required to counteract  
46 the increase in dilution rate inherent to faster proliferation and maintain average protein  
47 concentrations. This global coordination of gene expression with the division rate could

48 involve changes in transcription, translation and mRNA turnover. Experimental evidence  
49 suggests that in yeast and bacteria this coordination occurs primarily at the level of  
50 transcription (Keren *et al*, 2013; Gerosa *et al*, 2013; Berthoumieux *et al*, 2013; García-  
51 Martínez *et al*, 2016). Consistent with this, global translation rates in bacteria are less  
52 affected than transcription rates by the division rate, except at very slow proliferation rates  
53 (Klumpp *et al*, 2013; Dai *et al*, 2016). In *B. subtilis*, the translation rate (per mRNA) has  
54 even been found to decrease with the division rate, while the total mRNA concentration  
55 doubles as the division rate doubles (Borkowski *et al*, 2016). In yeast, mRNA turnover  
56 rates have been proposed to be globally regulated by the division rate (García-Martínez  
57 *et al*, 2016). Yet, it is unclear whether certain mechanisms of global gene expression  
58 regulation by the division rate are particularly advantageous over others for a fixed protein  
59 synthesis output.

60 The expression parameters of different genes do not necessarily follow the same dependency  
61 with the division rate. In fact, the proteome fraction of distinct functional classes has  
62 been shown to follow specific and simple trends with the division rate (Scott *et al*, 2010; Li  
63 *et al*, 2014; Hui *et al*, 2015). Fundamentally, for a given type of division rate modulation,  
64 proteins can be categorised in three classes ( $R$ ,  $P$ ,  $Q$ ) depending on whether their proteome  
65 fraction respectively increases, decreases or is maintained with the division rate. Simple  
66 models of proteome allocation and cell physiology have shown that the changes in global  
67 protein fractions observed experimentally are consistent with the maximisation of the  
68 division rate (Molenaar *et al*, 2009; Scott *et al*, 2014; Goelzer & Fromion, 2017). For  
69 example, when nutrient conditions are varied, ribosomal proteins that constitute most of  
70 the  $R$  proteins are needed in larger amounts to support fast growth in rich media (Scott  
71 *et al*, 2010). A consequence of a large  $R$  sector is that other proteins will necessarily fall  
72 into the  $P$  class, as proteome fractions add up to one. The  $Q$  class contains so-called  
73 housekeeping proteins, whose proteome fraction is maintained across all conditions.

74 Because total protein concentration is approximately constant across conditions (Basan *et*  
75 *al*, 2015), the concentration of  $P$  proteins decreases at fast growth. Lower concentrations  
76 mean lower number of molecules per unit of volume. Intrinsic noise, which results from the  
77 random timing of biochemical reactions and depends on absolute molecule numbers rather  
78 than concentrations, could therefore be higher at fast growth. Intrinsic noise contributes to  
79 cell-to-cell variability in gene expression, which leads to non-genetic phenotypic variability  
80 (Shahrezaei & Swain, 2008). In addition, gene expression is affected by *other* stochastic  
81 and dynamic cellular processes, resulting in so-called extrinsic noise (Elowitz *et al*, 2002;  
82 Shahrezaei *et al*, 2008). An important source of extrinsic noise in gene expression stems  
83 from the processes associated with the cell cycle, including cell growth and cell division,  
84 as illustrated by several experimental and modelling studies that are discussed below.  
85 Mathematical modelling has suggested that random partitioning of biomolecules at cell  
86 division is an important source of noise in gene expression and hard to separate from  
87 intrinsic noise (Huh & Paulsson, 2011). Other modelling studies have highlighted the  
88 contribution of heterogeneity in cell cycle time on noise in gene expression (Johnston *et al*,  
89 2012; Schwabe & Bruggeman, 2014; Antunes & Singh, 2014; Soltani *et al*, 2016). Also, cell  
90 cycle dependent expression and the timing of DNA replication also influences noise in gene  
91 expression in unexpected ways (Luo *et al*, 2013; Schwabe & Bruggeman, 2014; Peterson *et*  
92 *al*, 2015; Soltani *et al*, 2016). Several experimental studies have identified the cell cycle  
93 as a major source of noise in gene expression in bacteria and yeast (Cookson *et al*, 2010;  
94 Zopf *et al*, 2013; Keren *et al*, 2015; Walker *et al*, 2016). These studies suggest that gene  
95 expression noise is generally higher at lower division rates (Keren *et al*, 2015; Walker *et al*,  
96 2016). The impact of cell division and random partitioning of molecules on the behaviour  
97 of simple circuits has also been studied by modelling (Gonze, 2013; Lloyd-Price *et al*, 2014;  
98 Bierbaum & Klumpp, 2015). It has been shown that simple genetic oscillators can sustain  
99 oscillation in the presence of cell division but the oscillations could be entrained by the

100 cell cycle depending on the circuit topology (Gonze, 2013). Also, it is shown that random  
101 partitioning of biomolecules at division affects dynamics of simple circuits for example  
102 affecting stability of biological switches (Lloyd-Price *et al*, 2014).

103 Cell size is regulated both across the division cycles and between different growth conditions.  
104 Although this is a long-standing problem in cell biology, the mechanisms behind cell size  
105 homeostasis remain largely elusive. Interest for this question has been recently renewed,  
106 particularly in bacteria. Recent data suggests that many bacterial species follow a so-called  
107 adder principle, adding a constant cytoplasm volume in each division cycle, independently  
108 of their size at birth. Interestingly, cell size at division is positively correlated with division  
109 rates in both bacteria and yeast, cells becoming larger in richer environments (Schaechter  
110 *et al*, 1958; Turner *et al*, 2012). Although this is a universal observation, there is no  
111 satisfying universal explanation of why cells have evolved such regulation of cell size with  
112 growth conditions.

113 Global regulation of gene expression and cell size is likely to affect the dynamics and  
114 function of genetic and biochemical networks inside cells (Shahrezaei & Marguerat, 2015).  
115 A pioneering study quantified how division rate dependent global regulation of gene  
116 expression affects the average concentration of a constitutively expressed gene product,  
117 and how this in turn can affect the behaviour of simple synthetic genetic networks (Klumpp  
118 *et al*, 2009). Another theoretical study showed that the division rate dependence of gene  
119 expression could impact the qualitative behaviour of a synthetic oscillator circuit, the  
120 ‘repressilator’ (Osella & Lagomarsino, 2013). Moreover, the division rate regulation of a  
121 gene impacting fitness can result in non-trivial global feedback in gene regulation (Klumpp  
122 *et al*, 2009; Kiviet *et al*, 2014; Tan *et al*, 2009). However, theoretical insights on how global  
123 regulation of gene expression and cell size with growth conditions impacts noise in gene  
124 expression and therefore the behaviour of biochemical circuits are still largely lacking.

125 In this study, we shed light on the regulation of noise in gene expression across growth

126 conditions by integrating existing data in the bacterium *E. coli* on global regulation of gene  
127 expression and cell size into detailed computational models of stochastic gene expression  
128 in growing and dividing cells. We then use examples of some simple genetic networks to  
129 illustrate how the changes in gene expression noise across growth conditions affects the  
130 dynamics of cellular systems.

## 131 Results

### 132 Stochastic gene expression in growing and dividing cells

133 To fully capture the effect of cell cycle on noise in gene expression, we model the stochastic  
134 expression of a single gene in growing and dividing cells (Figure 2 A-B, Supplemental  
135 Figure 1-A). Transcription, mRNA degradation and translation are represented by single  
136 stochastic reactions. Corresponding rates are noted  $k_m$ ,  $\gamma_m$  and  $k_p$  respectively. Because  
137 the majority of *E. coli* proteins are stable, we first neglect protein degradation. During  
138 the cell cycle, we assume cell size increases exponentially at a fixed rate, that results in a  
139 decrease of the concentration of the mRNA and the protein when their numbers do not  
140 change. We model cell division as a discrete event that splits the cell volume in two, and  
141 each molecule is randomly partitioned between daughter cells with a probability matching  
142 their inherited volume fraction. In our simulations, we keep only one of the two daughter  
143 cells, therefore reproducing the popular *mother machine* experimental setting (Wang *et al*,  
144 2010).

145 Cellular growth rate, cell size at division, and cell size at birth are all known to vary  
146 between individual cells even in identical, tightly controlled conditions. Variability in size  
147 at birth arises from variability in the mother cell size at division but also from imperfect  
148 volume splitting between the two daughter cells. To realistically account for this variability,  
149 we use the *noisy linear map* (NLM) model (see Methods and Supplemental Figure 1), a



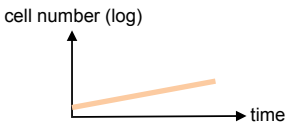
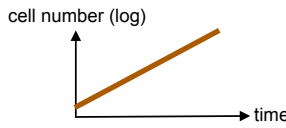

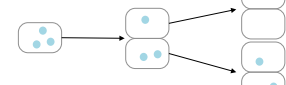
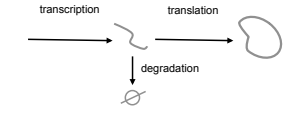
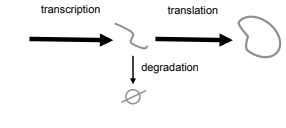
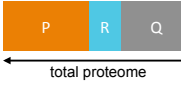
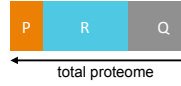


|                           |  |  |
|---------------------------|--|--|
| Nutrient Quality          | poor  | rich  |
| Population Doubling Rate  |       |        |
| Dilution and Partitioning |       |        |
| Gene Expression           |       |        |
| Proteome Allocation       |      |       |
| Cell Size                 |     |     |
| Expression Noise          | ?  | ?  |

Figure 1: **Global cellular factors affecting gene expression noise that depend on growth conditions.** Nutrient quality can increase the population doubling rate by promoting growth and division of individual cells. This leads to increased dilution of molecules, and more frequent random partitioning of molecules between daughter cells. Because faster growth requires a higher rate of cell mass production, rates of mRNA and protein expression increase globally with the division rate. However, the relative changes in mRNA and protein expression rates is gene-dependent because the proteome composition is reshaped when the division rate changes (Scott *et al*, 2014). For example, the fraction of ribosomal proteins (*R* proteins) will increase with the division rate while the fraction of metabolic enzymes (and other *P* proteins) will decrease, the fraction of house keeping proteins (and other *Q* proteins) remain constant (Scott *et al*, 2010). Cell size as well is known to increase with the division rate in response to nutrient-based modulations (Schaechter *et al*, 1958; Basan *et al*, 2015). All those factors affect both average expression and expression noise in a non-trivial manner.

150 recent phenomenological model of cell size control that captures the variability in cell  
151 size at birth and division observed experimentally as well as their correlation within  
152 individual cell cycles (Tanouchi *et al*, 2015; Jun & Taheri-Araghi, 2015). The degree of  
153 this correlation is related to the mechanisms underlying cell size homeostasis. For example,  
154 a noisy linear map with the parameter  $a$  equal to 1 corresponds to an adder strategy,  
155 where a fixed cytoplasm volume is added to the cell between each division. Alternatively,  
156 a parameter  $a$  equal to zero corresponds to a sizer strategy, where cell division is triggered  
157 at a fixed size (Jun & Taheri-Araghi, 2015).

158 A priori, it is possible that the NLM parameters that best describe a given single-cell  
159 dataset could change with growth conditions. Therefore, we have inferred the parameters  
160 of the NLM from a recent mother machine dataset of cells grown in 7 different carbon  
161 sources supporting a wide range of division rates (Taheri-Araghi *et al*, 2015). We find  
162 that NLM parameters can indeed change with the division rate (Supplemental Figure  
163 1). As expected,  $b$  strongly increases with the division rate (the average size at division  
164 is given by  $\frac{2b}{2-a}$ ). Notably, the slope parameter  $a$  is significantly lower than 1 at slow  
165 growth, consistently with another study reporting a deviation towards a sizer strategy  
166 ( $a < 1$ ) in slow regimes (Wallden *et al*, 2016). In addition, individual cell growth rates  
167 are well described by normal distributions in all conditions. Based on that analysis, we  
168 derive linear functions describing all NLM parameters as a function of the division rate  
169 (Supplemental Figure 1). This enables us to realistically model growth and division at the  
170 single cell level over a wide range of division rates and investigate their effects on gene  
171 expression noise.

172 Before starting to explore effect of division rate on noise in gene expression and using the  
173 NLM parameters extracted from the data, we first explore the effect of these parameters  
174 on the gene expression noise for a fixed growth condition, as this has not been explored  
175 before. In Figure 2-C, we show protein number and concentration noise (CV) at cell



176 birth (immediately after cell division and at the beginning of the cell cycle) as the noise  
177 in final size ( $\sigma_1$ ), noise in size partitioning ( $\sigma_2$ ) and  $a$  are varied. Large noise in NLM  
178 noise ( $\sigma_1$  or  $\sigma_2$ ) results in an increased noise in protein number noise at the beginning  
179 of the cell cycle (Figure 2-C). This is due to partitioning noise as this increased protein  
180 number noise is mostly decayed in the middle of cell cycle (Supplemental Figure 2). Also,  
181 protein concentration noise is not so much affected by NLM noise as we assume probability  
182 of random partitioning of biomolecules is proportional to the inherited volume of the  
183 daughter cells after division. For values of  $a$  greater than one size control is not very  
184 effective in filtering noise in cell size and there is an increased size variability for large  $a$   
185 and large NLM noise ( $\sigma_1$  or  $\sigma_2$ ) (Modi *et al*, 2017). As a result the protein concentration  
186 noise that directly depends on cell volume shows an increase at large  $a$  and large NLM  
187 noise. Overall, these results show that the physiological range of NLM parameters across  
188 growth conditions (Supplemental Figure 1) are not expected to produce strong effects in  
189 noise gene expression.

190 In the results shown in Figure 2-C, we have assumed the reaction propensities for tran-  
191 scription, translation and mRNA decay are independent of cell volume. In Supplemental  
192 Figure 3, we show the impact of a cell size-dependent transcription rate. Interestingly,  
193 in this case, the protein concentration noise is reduced and becomes independent of the  
194 NLM parameters. We obtain very similar results if we assume translation rate is size-  
195 dependent (not shown). Size dependence of transcription rate has been recently reported  
196 in eukaryotes (Padovan-Merhar *et al*, 2015; Kempe *et al*, 2015), while similar evidence in  
197 prokaryotes is lacking. Therefore, in this work we assume cell size independent propensities  
198 for all first-order reactions (but volume dependency for bi-molecular reaction propensities  
199 is accounted for). Also, we focus on protein *concentration* noise (physiologically more  
200 relevant than molecule numbers) and across newly born cells (to eliminate cell cycle stage  
201 contributions, similar trends are seen in the middle of the cell cycle).

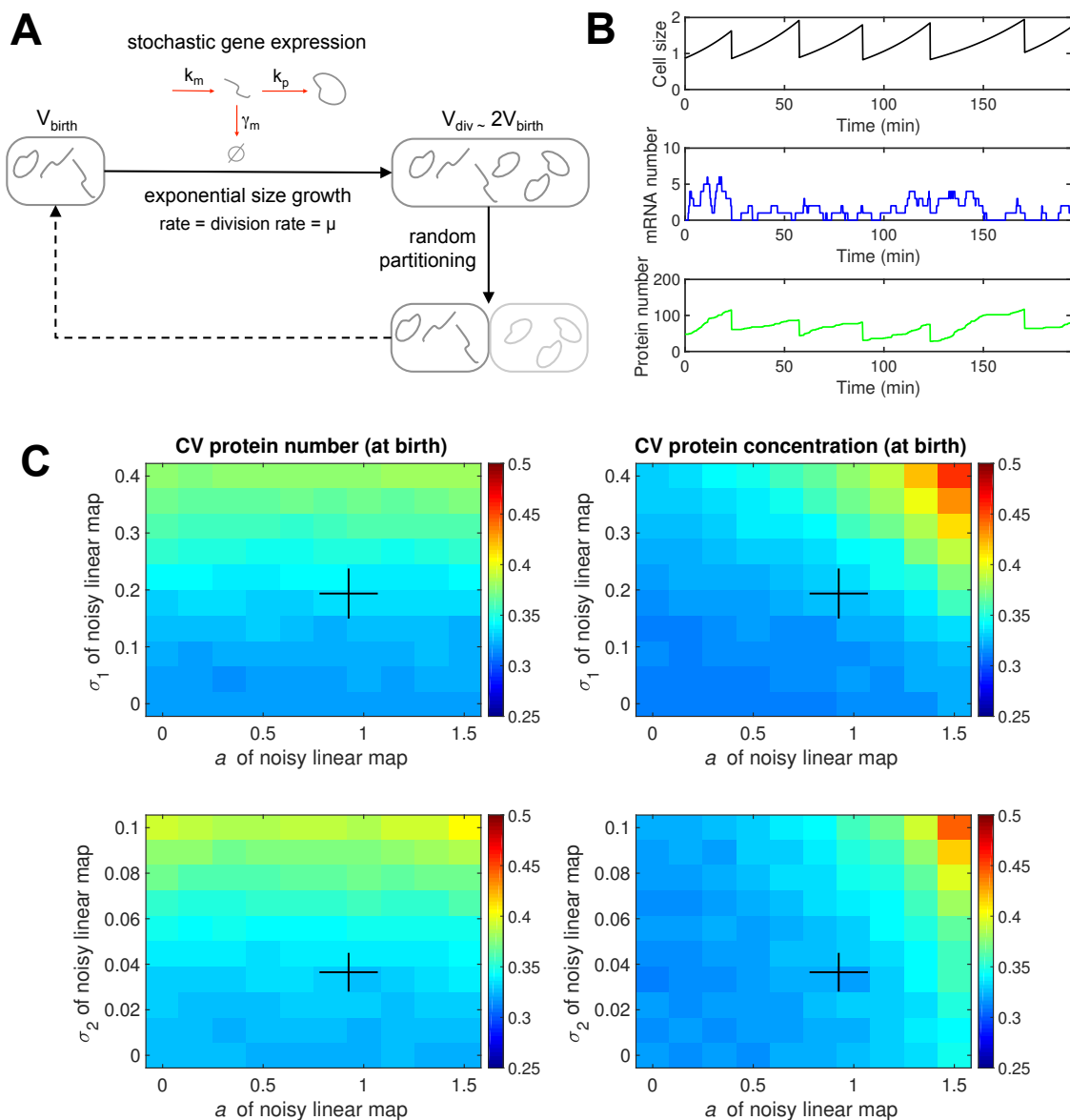


Figure 2: **Modelling stochastic gene expression in growing and dividing cells.** (A) Sketch of the modelling approach. See Methods for details. (B) Example of simulated trajectories. Typical parameters for *E. coli* have been used (see Methods). (C) Impact of noisy linear map (NLM, see Methods) parameters on protein noise. Heatmaps of protein number noise (left) or concentration noise (right) (defined as the coefficient of variation, CV, across newly born cells) when  $a$  and  $\sigma_1$  (top) or  $a$  and  $\sigma_2$  (right) are varied. Other parameters are kept constant at reference values, except  $b$  that changes with  $a$  such that the average size at birth is constant. Black crosses indicate empirical ranges estimated from mother machine data (see Methods and Supplemental Figure 1).

202 **Expression noise depends on division rate even when protein concentration is**  
203 **maintained**

204 We consider first genes whose protein concentration stays constant when the division rate  
205 changes (i.e. proteins belonging to the  $Q$  class). Interestingly, this requires that at least  
206 one of the gene expression rates  $k_m$  (transcription rate),  $\gamma_m$  (mRNA degradation rate) or  
207  $k_p$  (translation rate per mRNA) changes with the division rate to compensate for increased  
208 dilution of mRNA and protein molecules.

209 Using our model and typical values for gene expression rates at 2 doublings per hour  
210 as a baseline, we computed the change in protein concentration *noise* with the division  
211 rate when average concentration is maintained either by adapting the transcription rate  
212 only (Figure 3-A) or the translation rate per mRNA only (Figure 3-B). To investigate  
213 the contribution of distinct sources of noise and of variability in cell size to protein  
214 concentration noise we consider multiple scenarios in which different sources of variability  
215 are turned off (colour codes in Figures 3-A and 3-B).

216 Our simulation results reveal that maintaining average protein concentration by adjusting  
217 transcription or translation to the division rate leads to very different behaviours of the  
218 protein concentration noise. We find that the empirically observed increase of cell size with  
219 division rate strongly contributes to these behaviours. In the case of transcription rate  
220 adjustment, protein noise sharply decreases with the division rate. A milder decrease is  
221 also observed when cell size is kept constant across division rates. In the case of translation  
222 rate adjustment, protein noise increases with the division rate instead, whether cell size  
223 changes or not.

224 To better understand these results, we looked at how mRNA numbers change with the  
225 division rate in the different situations (bottom left plots in Figures 3-A and 3-B). When  
226 transcription adjusts to the division rate in order to maintain average protein expression,

227 mRNA numbers increases with the division rate. As mRNA noise (mRNA numbers are  
228 typically much lower than protein numbers) is a major contributor of protein noise, an  
229 increase in mRNA numbers results in a decrease in protein noise. However when instead  
230 translation adjusts to the division rate, mRNA numbers remain mostly unchanged. This  
231 is possible, because mRNA degradation rates are large compared to the division rate,  
232 resulting in mRNA numbers being less sensitive to dilution than protein numbers. Despite  
233 little change in mRNA numbers and hence mRNA noise, the increase in protein noise can  
234 be explained by a higher propagation of the mRNA noise to protein, since contribution of  
235 transcription to protein noise depends on the ratio of mRNA lifetime (which is mostly  
236 constant) and protein lifetime (which is set by the dilution rate, itself set by the division  
237 rate) (Swain *et al*, 2002).

238 While the relative contribution of distinct noise sources (stochastic gene expression,  
239 partitioning noise, variability in cell growth rate, cell division size and cell birth size) to  
240 total protein noise can change with the division rate, we find that the contribution of  
241 stochastic gene expression is predominant at all division rates (Supplemental Figure 4). For  
242 the case of transcription adjusting to division rate, we find the contribution of partitioning  
243 noise is relatively constant across division rates, while contribution of LNM noise increases  
244 several folds at fast division rates. In contrast for the case of transcription adjusting to  
245 division rate, we find the contribution of partitioning noise significantly decreases at fast  
246 division rates, while contribution of LNM noise remains relatively constant.

247 In summary, our simulations demonstrate that for genes with typical expression parameters  
248 at intermediate division rates, maintaining a constant protein concentration across growth  
249 conditions by adjusting transcription to the division rate leads to a decrease of protein  
250 noise. In contrast, adjusting translation to the division rate increases protein noise levels.

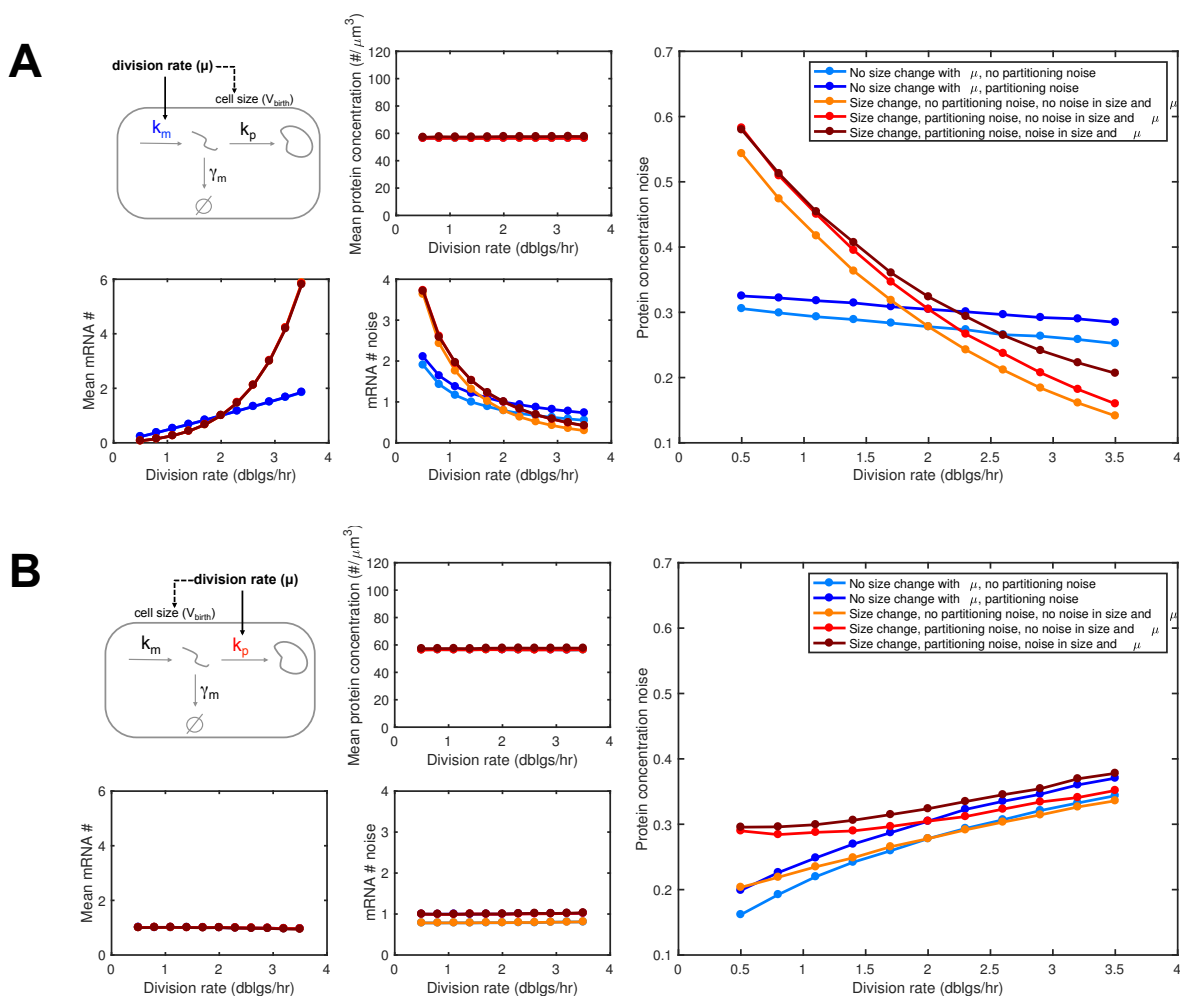


Figure 3: **Changes in cell size, transcription and translation rates with the division rate impact expression noise even when average protein concentration is maintained ( $Q$  expression).** (A) Change of protein concentration noise (right) with division rate when the average concentration is maintained (middle-top plot) by tuning the transcription rate (left-top plot). Noise is the CV of protein concentration across newly born cells. The mRNA average number ( $\#$ ) and CV in are also shown (bottom-left plots). Different model variants are simulated to explore the contribution of random partitioning noise, size change with the division rate, and noise in size (NLM parameters) and cellular growth rate (see Methods and Supplemental Figure 1). (B) Same as (A) but when the translation rate is tuned instead of the transcription rate.

251 **Increase of cell size with the division rate prevents noise increase for consti-**  
252 **tutively expressed proteins despite a decrease in average concentration**

253 The results described above concern proteins belonging to the  $Q$  category, whose average  
254 concentration is maintained constant independently of the division rate. Klumpp and  
255 colleagues have shown that constitutively expressed proteins instead belong to the  $P$   
256 category: their concentration is decreased at fast growth (Klumpp *et al*, 2009). The  
257 transcription rate of constitutively expressed genes strongly increases with the division  
258 rate, while mRNA degradation rate and translation rate per mRNA remain relatively  
259 constant (Klumpp *et al*, 2009). However, this is not sufficient to balance both increased  
260 dilution and increased cell size (Klumpp *et al* (2009), Supplemental Figure 5 and Figure 4  
261 top left plot).

262 Remarkably, using parameters of gene expression from (Klumpp *et al*, 2009) (see Methods  
263 and Supplemental Figure 5), we find that protein noise decreases with division rate, despite  
264 the strong decrease in average protein concentration (Figure 4). Cell size increase with  
265 division rate is a key contributor to this behaviour. Assuming that increased expression  
266 noise for  $P$  proteins at fast growth is deleterious, this observation could explain why  
267 increased cell size at fast division rates is a universally conserved feature of unicellular  
268 organisms.

269 In the case of a  $P$  protein, similarly to the case of  $Q$  protein above, we find that the relative  
270 contribution contribution of stochastic gene expression is predominant at all division rates  
271 (Supplemental Figure 4). However, contribution of both partitioning noise and size and  
272 growth rate variability increases moderately at fast division rates.

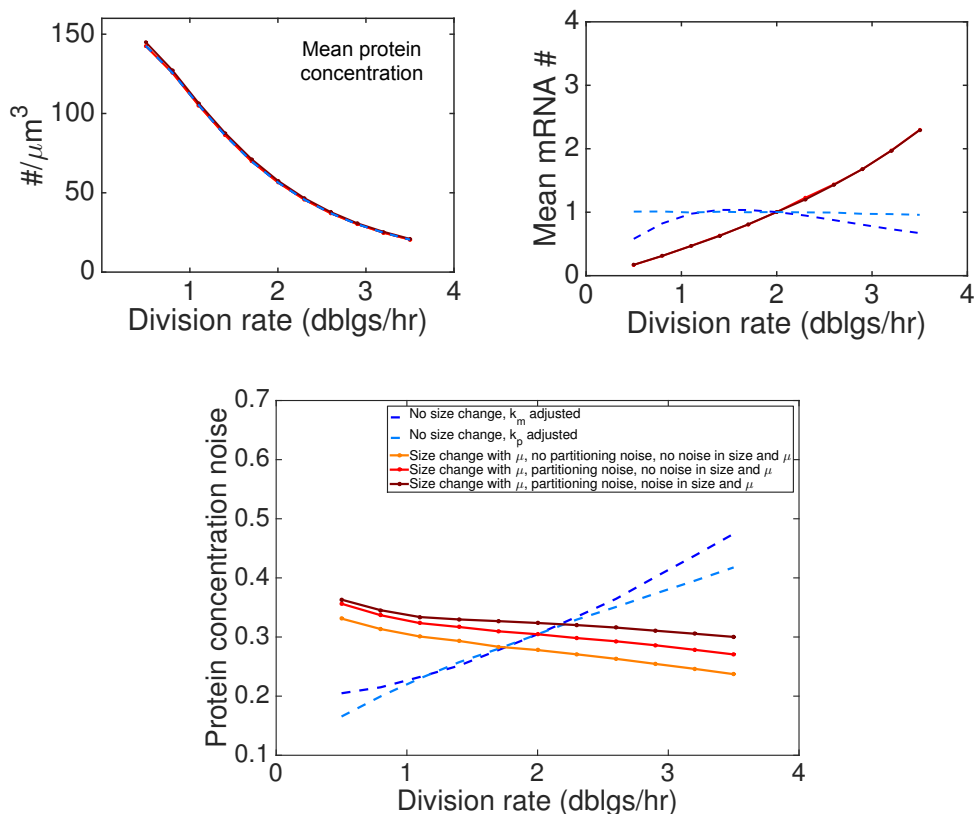


Figure 4: **Larger cell size at fast division rates prevents expression noise increase despite a decrease in average concentration ( $P$  expression).** To reproduce  $P$  expression, we used gene expression parameter dependencies with division rate for constitutively expressed proteins extracted from a previous study ((Klumpp *et al*, 2009), see Methods and Supplemental Figure 3 for details). Average protein concentration (top left), average mRNA number (#) (top right) and protein concentration noise (bottom) are shown. The same model variants as in Figure 3 were used. Two additional scenarios are also shown, in which cell size does not change with division rate but either the transcription rate (dashed dark blue) or the translation rate (dashed light blue) is adjusted to obtain the same decrease of average protein concentration with division rate (other parameters remaining constant and equal to the reference values of solid line simulations at 2 doublings per hour).

## 273 Impact of division rate on the behaviour of an oscillator circuit

274 Changes in average expression and noise of individual proteins with the division rate in  
275 response to environmental changes is likely to impact the behaviour of genetic circuits  
276 (Klumpp *et al*, 2009). Even when the protein average expression (in isolation, i.e. without  
277 the circuit-specific regulations) is maintained, the expression noise can still change (Figure  
278 2) meaning that circuit behaviour could depend on the division rate (Shahrezaei &  
279 Marguerat, 2015).

280 To investigate these effects, we first consider a two proteins oscillator circuit recapitulating  
281 essential features of circadian clocks (Figure 5-A) (Vilar *et al*, 2002). An actively degraded  
282 activator protein ( $A$ ) promotes its own transcription as well as the transcription of a  
283 stable repressor protein ( $R$ ) by promoter binding.  $R$  can also binds  $A$ , preventing it  
284 to bind promoters. This circuit can lead to oscillations as illustrated in Figure 5-B. A  
285 detailed analysis of why oscillations arise is beyond the scope of this study and has been  
286 explored before (Guantes & Poyatos, 2006; Kut *et al*, 2009). Briefly, because  $R$  competes  
287 with promoters for the binding of  $A$ , when the amount of free  $R$  is large only basal  
288 transcriptional activity for both genes is possible. Because  $R$  is stable, such a state can last  
289 until dilution and partitioning renders free  $R$  levels too low to efficiently prevent promoter  
290 binding by  $A$ . Promoter activation leads to a burst of  $A$  by auto-activation, but  $R$  levels  
291 eventually rise because  $A$  also promotes  $R$  transcription. When  $R$  levels are sufficient to  
292 efficiently compete with  $A$  promoter binding, a novel cycle starts.

293 We asked how the circuit behaviour was affected when division rate modified. We first  
294 assume that basal transcription, translation and mRNA degradation follows the same  
295 dependency as constitutively expressed proteins (i.e.  $P$  proteins, as in Figure 4), and  
296 that the fold-change increase of transcription rate when the promoter is activated by  
297  $A$  is independent of the division rate. The resulting changes in circuit behaviour with



298 the division rate are shown in Figure 5-C (black lines). The average period increases  
299 as the division rate decreases because dilution is an important driver of the oscillations.  
300 The average amplitude of free  $R$  oscillations is also strongly dependent on the division  
301 rate, and decreases as the division rate increases. This is consistent with  $P$  expression,  
302 although different behaviours are in theory possible because of gene regulation. The noise  
303 in circuit behaviour changes as well with the division rate. Specifically, noise in period  
304 and amplitude of the oscillations display ‘U’ shape dependencies with the division rate,  
305 with lower noise close to the reference division rate of 2 doublings per hour. In summary,  
306 constitutive expression (typical of  $P$  proteins) leads to changes in average behaviour and a  
307 strong increase in noise of an oscillatory circuit at very low or very high division rates.

308 We then investigated whether  $Q$  expression of the circuit components could increase the  
309 robustness of oscillations in response to changes in division rate. As in Figure 3 we consider  
310 two modes of  $Q$  expression, either by transcriptional adjustment (blue) or translational  
311 adjustment (red). Both modes could maintain the average amplitude of oscillations in a  
312 narrow range, but the average period remained strongly dependent on the division rate  
313 (Figure 5-C). While both modes resulted in identical changes in circuit average behaviour,  
314 they led to slightly different dependencies of noise in oscillations with the division rate.  
315 The division rate with the minimal noise in amplitude is around 2.3 doublings per hour for  
316 transcriptional adjustment and around 1.5 doublings per hour for translational adjustment.  
317 In summary,  $Q$  expression increased robustness of oscillations compared to constitutive  
318 ( $P$ ) expression, but it is not sufficient to make the oscillator’s period independent of the  
319 division rate.  $Q$  expression via transcriptional or translational adjustment led to similar,  
320 but not identical changes of noise in oscillations with the division rate.

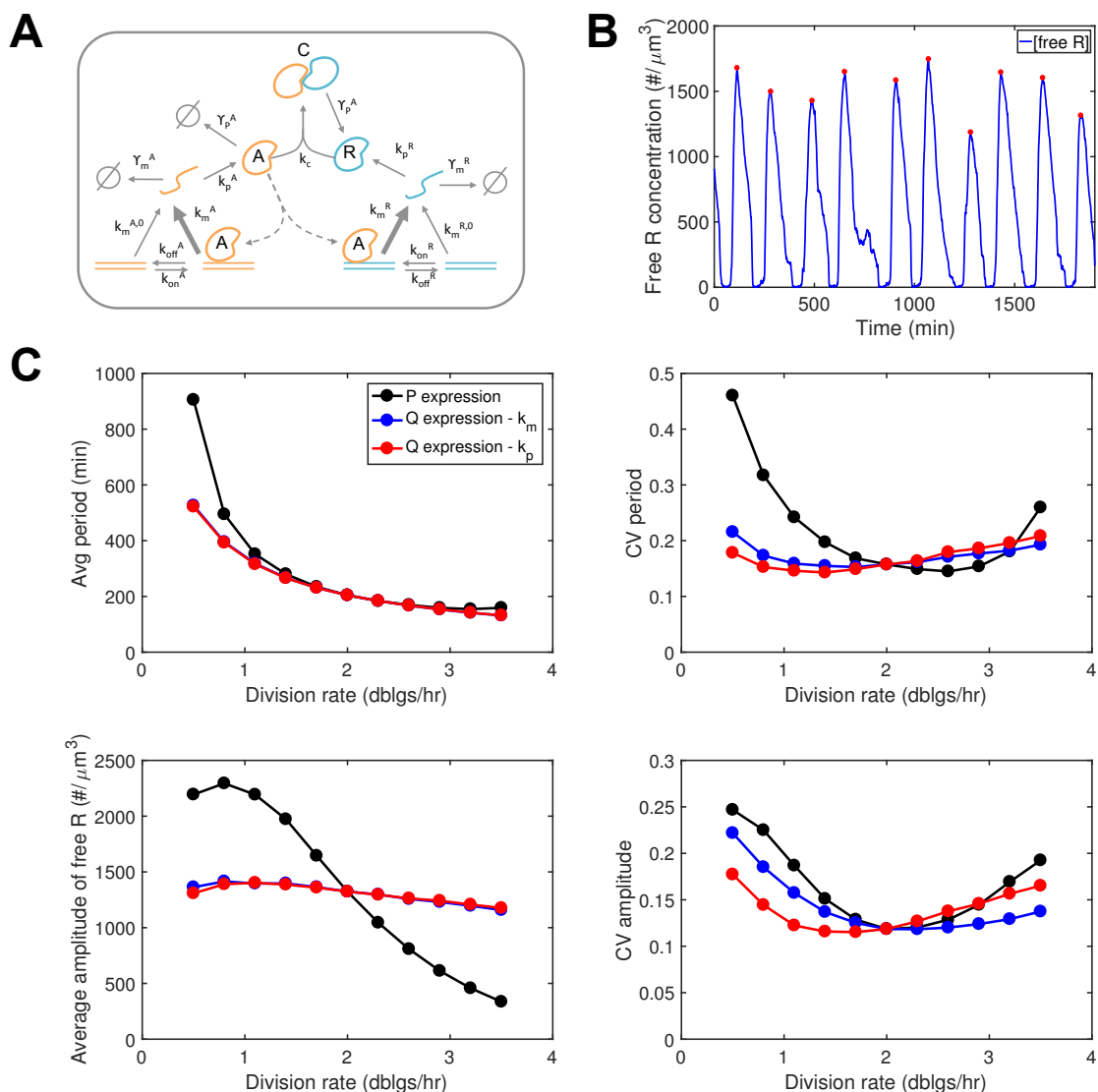


Figure 5: **Behaviour of an oscillator circuit at different division rates.** (A) Schematic of the oscillator circuit described in (Vilar *et al*, 2002). See methods for model description and parameter values. (B) Example simulation showing oscillations in free R concentration. Detected peaks are shown with red circles. Note that the timescale of oscillations is around 3 hours, while the inter-division time is around 30 minutes. (C) Change of the oscillatory behavior (average period, noise in period, average amplitude, noise in amplitude) as a function of division rate. The black curves correspond to P expression. The other curves correspond to situations in which either transcription rates (blue) or translation rates (red) are increasing with division rate in order to maintain average expression (Q expression in absence of binding of A with R).

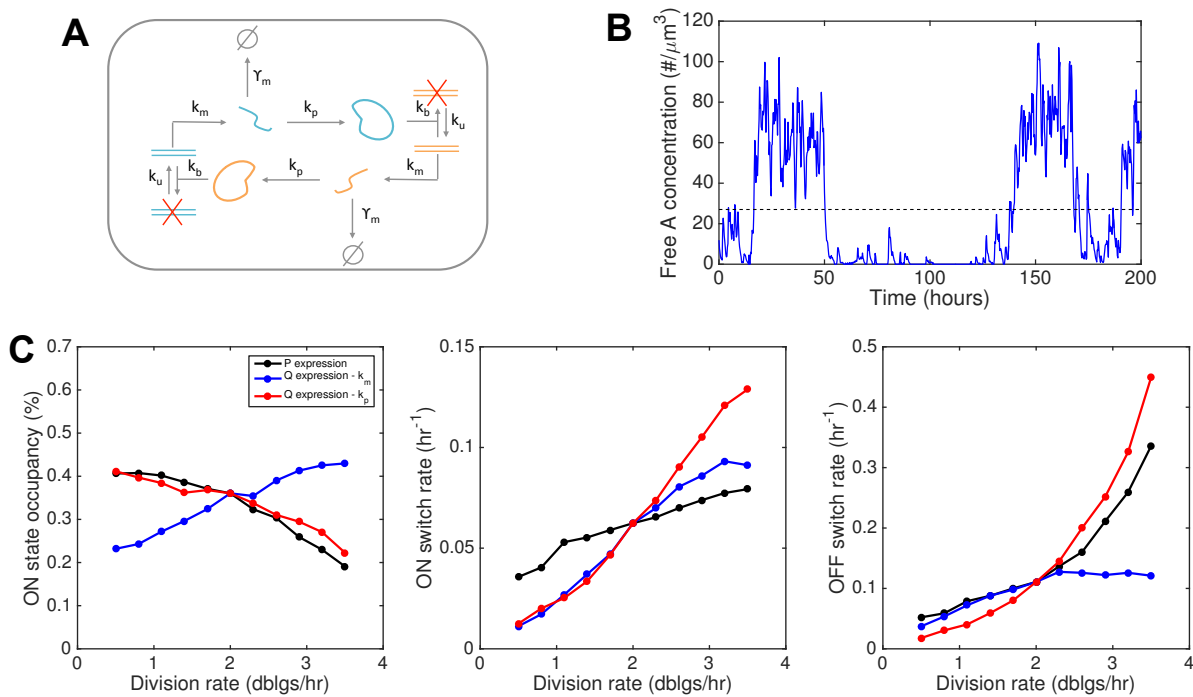
## 321 Impact of division rate on the behaviour of the toggle switch

322 We investigate next a simple synthetic circuit known to exhibit bistability: the toggle  
323 switch (Gardner *et al*, 2000), in which two proteins repress each other's transcription  
324 (Figure 6-A). We asked first whether different circuit behaviours, namely the existence  
325 of bistability, the occupancy of the states, and the switching rates between states, were  
326 affected by changes in division rate and adjustment of transcription or translation to  
327 division rates. To this end, we consider simple model assumptions that are sufficient to  
328 generate stochastic switching between different states (Methods) with typical parameter  
329 values.

330 We found that the circuit could exhibit bistability (Figure 6-B,C) over the considered  
331 range of division rates for constitutive ( $P$ ) expression as well as for  $Q$  expression by  
332 transcriptional or translational adjustment. However, in all cases the circuit behaviour  
333 strongly depends on the division rate (Figure 6-C), as illustrated by the change in  $ON$   
334 state occupancy (the circuit is  $ON$  when one of the two proteins, the reporter, is in  
335 the high expression state). Interestingly, the change of behaviour is very different for  
336 different modes of  $Q$  expression: for translational adjustment, the  $ON$  state occupancy  
337 decreases with the division rate (in a fashion very similar to  $P$  expression). However, an  
338 opposite behaviour is observed for  $Q$  expression via transcriptional adjustment as  $ON$   
339 state occupancy becomes positively correlated with division rate..

340 The  $ON$  state occupancy reflects the balance between stochastic switching in and out of  
341 this state. These rates are both dependent on the division rate (Figure 6-C, middle and  
342 right plots). We find that the switching rates increase with the division rate that could  
343 suggest random partitioning of mRNA and protein molecules, which is more frequent at  
344 high division rates, favours switching as also reported in another study (Lloyd-Price *et*  
345 *al*, 2014). In addition, the observation that at fast growth the  $OFF \rightarrow ON$  rate rises the

346 most sharply for  $Q$  expression via translational adjustment is consistent with the high  
 347 level of protein noise for this mode of regulation at fast division rates (Figure 3-B).



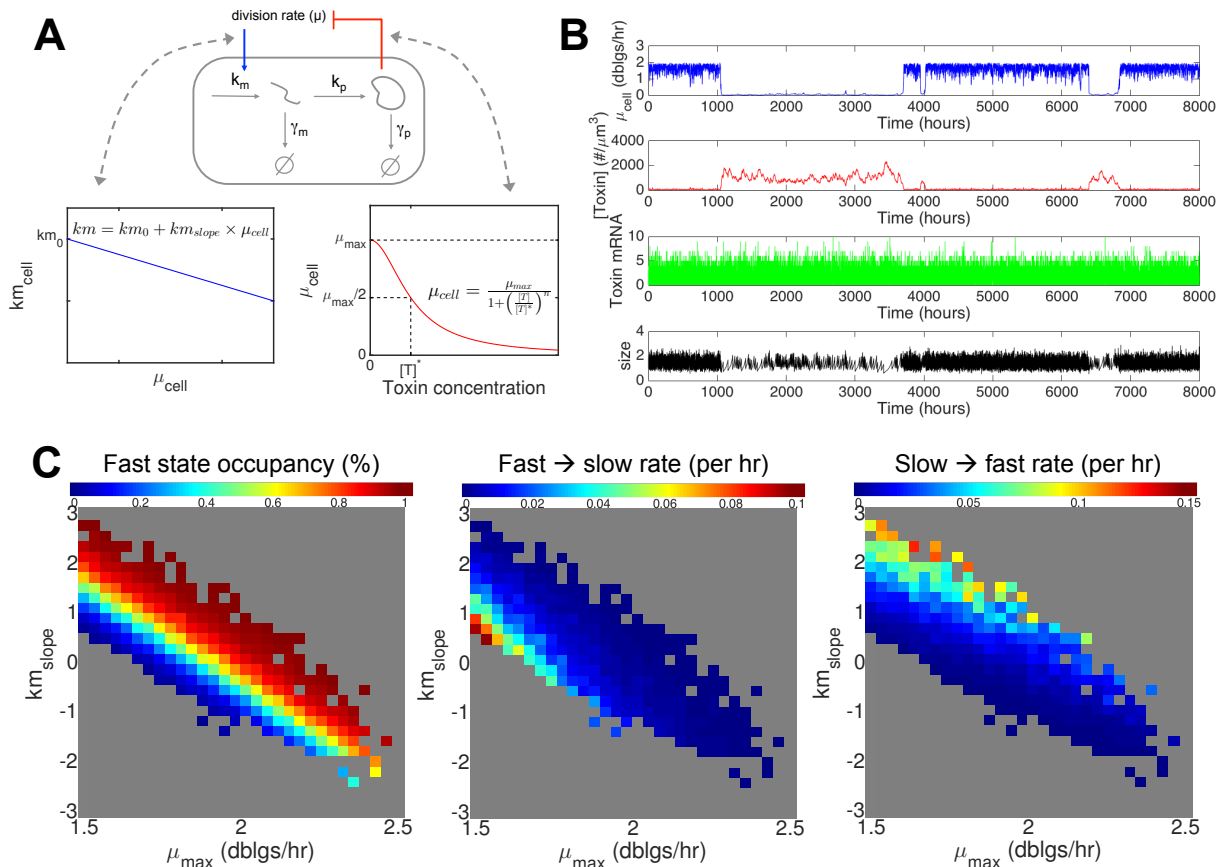
**Figure 6: Behaviour of the toggle switch at different division rates.** (A) Schematic of the toggle-switch circuit. Two proteins  $A$  and  $B$  can transcriptionally repress each other by promoter binding. (B) Example simulation of the toggle-switch circuit functioning in growing and dividing cells, showing stochastic switching between high ( $ON$ ) and low ( $OFF$ ) expression for one protein. The threshold separating the two states (black dashed line) is computed using the overall protein distributions (see Methods). (C) Change of the toggle-switch behaviour, quantified by the average time spent in the  $ON$  state and the switching rates between the two states, as a function of division rate. The black curve corresponds to  $P$  expression as in Figure 3, the blue and red curves corresponds to constant average expression maintained either transcriptionally or translationally, as in Figure 2-C,D. Note that when the concentration of one protein type is low, the other is not necessarily high. This is why the  $ON$  state occupancy is not always 50% despite the symmetry between the two proteins.

348 **When gene expression feedbacks on growth: the case of toxin-mediated**  
349 **growth inhibition**

350 So far, the circuits we have considered respond to changes in division rate but they don't  
351 impact cell physiology and growth. However, many natural circuits and some synthetic  
352 circuits do influence cell physiology, for example by regulating cell metabolism or cell cycle  
353 progression. Even when synthetic circuits are not designed to impact cell physiology, they  
354 often do by competing with core cellular processes for global cellular resources, and this  
355 has become a major concern for synthetic biologists (Ceroni *et al*, 2015).

356 In prokaryotes, well-known examples of gene expression feeding back on growth are toxin-  
357 antitoxin systems. These systems are involved in bacterial persistence, where a very small  
358 subpopulation of slow growing cells naturally arises among a normally growing population.  
359 A minimal model, where a single protein is toxic for growth was found to be sufficient to  
360 generate growth bistability (Klumpp *et al* (2009), Tan *et al* (2009), Rocco *et al* (2013),  
361 and Figure 7-B). Here we investigate the behaviour of this kind of model (Figure 7) when  
362 both the maximal growth rate reached by a toxin-free cell and the dependency of the  
363 transcription rate with the cell growth rate are varied.

364 For each parameter set enabling growth bistability (coloured pixels in Figure 7-C), we  
365 computed the occupancy of the fast state (Figure 7-C, left) and the switching rates between  
366 the slow and fast states (Figure 7-C, middle and right). The occupancy of the fast growing  
367 state decreases when the maximal growth rate decreases (Figure 7-C, moving from right to  
368 the left), and this behaviour is independent of the dependency of the toxin transcription  
369 rate to the cell division rate (i.e. the value of  $km_{slope}$ ). Therefore, the system will naturally  
370 respond to less favourable growth conditions by increasing the time spent in the slow state.



**Figure 7: Growth bistability caused by expression of a toxic protein. (A)** Model description. The instantaneous cell growth rate, which here we assume to be a decreasing function of the expressed protein concentration. In turn, changes in cell growth rate impacts gene expression via the transcription rate. **(B)** Growth bistability is possible with realistic parameter values (Methods). In the simulation shown,  $k_{m_{slope}} = 0$ , meaning that the positive feedback: toxin  $\rightarrow$  slower growth  $\rightarrow$  more toxin is only mediated by changes in dilution. **(C)** Influence of growth conditions ( $\mu_{max}$ ) and growth rate dependence of transcription ( $k_{m_{slope}}$ ) on growth bistability. For each parameter set,  $k_{m_0}$  was also adjusted such that  $k_{m_{cell}}(2 \text{ doublings/hr}) = 0.28 \text{ min}^{-1}$ . From corresponding simulations, the existence of bistability was tested and corresponding switching rates were estimated (See Methods).

## 371 Discussion

372 In this study, we have used detailed simulations of stochastic gene expression in growing  
373 and dividing bacteria to investigate the role of division rate in protein noise and dynamics  
374 of genetic networks. Our simulations are constrained by data available for *E. Coli* related to  
375 division rate regulation of constitutive gene expression (Klumpp *et al*, 2009) and single-cell  
376 data related to cell size control (Taheri-Araghi *et al*, 2015). For a constitutively expressed  
377 gene, we find that coupling transcription but not translation to division rate results in lower  
378 protein noise levels. Interestingly, existing data seem to suggest that global regulation of  
379 gene expression with division rate mostly acts at the level of transcription (Keren *et al*,  
380 2013; Gerosa *et al*, 2013; Berthoumieux *et al*, 2013; García-Martínez *et al*, 2016), consistent  
381 with the idea that lower noise levels are beneficial, or even necessary, at fast growth.  
382 However, regulation at the level of translation has also been observed (Borkowski *et al*,  
383 2016), which, coupled to transcriptional regulation, could result in non-trivial interplay in  
384 terms of gene expression noise regulation.

385 An important factor that helps to minimise noise in gene expression at fast division  
386 rate is increased cell size. Large cell sizes in growth conditions with fast division rate  
387 results in higher overall number of mRNA and protein molecules, and reduce noise in gene  
388 expression. This is particularly relevant for the regulation of noise in gene expression for  
389 proteins belonging to *P* category (Figure 1) as their concentration go down at high division  
390 rates. Based on these results, we propose a possible evolutionary reason for microbial cells  
391 (bacteria and yeast) to grow bigger at fast growth is to reduce gene expression noise, which  
392 is presumably more detrimental to fitness at fast growth (Shahrezaei & Marguerat, 2015).  
393 At the mechanistic level, the division rate regulation of cell size could be implemented  
394 via the division rate regulation of gene expression for proteins involved in cell size control  
395 (Basan *et al*, 2015; Bertaux *et al*, 2016).

396 Our simulations included physiologically relevant levels of partitioning noise, size variability  
397 and growth variability. Overall, we observe that the contribution of these factors to protein  
398 noise is small but that it tends to vary with the division rate for the different cases  
399 considered. We also observed the noise in molecular numbers and concentrations do not  
400 always behave similarly, as the later directly depends on cell volume. Interestingly, we find  
401 that if transcription rate scales with cell size as recently reported in eukaryotes (Padovan-  
402 Merhar *et al*, 2015; Kempe *et al*, 2015), the concentration noise becomes independent of  
403 noise in cell size control mechanism. In bacteria, there has not been a careful investigation  
404 of transcription scaling with cell size and in the absence of such reports we have assumed  
405 cell size independent reaction propensities throughout this study. We also did not model  
406 the contribution of DNA replication to protein concentration noise, but its impact has  
407 been found experimentally to be very small (Walker *et al*, 2016).

408 We then tested how dynamics of simple biochemical networks respond to division rate.  
409 As shown by the seminal work of Klumpp *et al* (2009), we find overall that division rate  
410 regulation of concentration of  $P$  proteins can change the average behaviour of biochemical  
411 networks significantly. But, as discussed below, we find that even when proteins in  
412 the network have a  $Q$  regulation, the changes in noise properties of the individual gene  
413 expression can significantly alter the mean and noise properties of the system.

414 In the case of a genetic oscillator, we find changes in gene expression and cell size  
415 with the division rate can impact the behaviour of oscillatory circuits in a non-trivial  
416 manner. Namely, large changes of average expression with the division rate for constitutive  
417 expression ( $P$ ) of circuit components render circuit behaviour sensitive to the division  
418 rate. However, maintaining constant expression of circuit components (for example via  
419 transcriptional or translational adjustment) does not guarantee full robustness of circuit  
420 behaviour against changes in division rate. Robustness might require more complex, circuit-  
421 specific dependencies of gene expression with the division rate, or even specific circuit



422 architecture (Paijmans *et al*, 2016). Interestingly, we observed a ‘U’ shape dependency of  
423 noise on division rate suggesting that there could be an optimally robust growth condition  
424 for a specific network design and parameter combination, which is relevant to appropriate  
425 function of natural biochemical systems or synthetic systems.

426 The toggle switch circuit behavior is strongly dependent on the division rate and on the  
427 type of gene expression dependency with the division rate. So, this suggests the simple  
428 toggle switch circuit is not going to perform robustly across growth conditions. As for the  
429 oscillator circuit, maintaining average expression is not sufficient to generate a division rate  
430 independent behaviour. Moreover, this example shows that even when average expression  
431 is maintained, whether it is maintained via adjustment of transcription or translation  
432 matters, as the circuit behaves differently in either situation.

433 In the case of simple models of persistence induced by the expression of a toxic protein in  
434 single growing and dividing cells, we could investigate the impact of growth conditions  
435 and gene expression dependency with the cell growth rate on the emergence of growth  
436 bistability. The role of growth conditions in prevalence of persister cells is a very relevant  
437 problem as the growth conditions of bacteria during infection are likely to be altered by  
438 the immune system and therapeutic treatments for instance. So, to validate our simple  
439 modelling results, it would be interesting to assess quantitatively, if and how growth  
440 conditions regulate the probability of the non-growing persistence phenotype.

441 In molecular systems biology, we use models of biochemical networks to validate our  
442 mechanistic understanding of the system under study. We propose that such models  
443 should be tested also against data collected across cellular division rates. If the behaviour  
444 of the system is observed to be robust to growth conditions, then our models should be  
445 able to capture this robustness. Conversely, describing the ways in which the system  
446 behaviour changes across growth conditions is key to refine our models and therefore our  
447 mechanistic understanding of the system under study.

448 In synthetic biology, we often desire to build a system that either functions robustly at  
449 a particular growth condition or across a range of growth conditions. Our study shows  
450 that stochastic models of synthetic biochemical networks in growing and dividing cells  
451 coupled with data on the regulation of gene expression across division rates are essential  
452 to optimal design of system topologies that achieve robustness against changes in cellular  
453 division rates.

## 454 **Acknowledgments**

455 We would like to thank Philipp Thomas and Marc Sturrock for feedback on our manuscript  
456 and members of the Marguerat and Shahrezaei groups for discussions. We thank Suckjoon  
457 Jun for sharing the *E. coli* size data across growth conditions. We acknowledge Matthew  
458 Robb for his preliminary work on this project during his PhD. This work is supported  
459 by a Leverhulme Research Project Grant (RPG-2014-408) awarded to SM and VS. SM is  
460 supported by the UK Medical Research Council.

## 461 **Methods**

### 462 **Modelling**

463 We describe here our basic model for gene expression in growing and dividing cells.  
464 mRNA molecules are randomly synthesized and degraded at rate  $k_m$  and  $\gamma_m$  respectively.  
465 Stochastic synthesis of protein from each mRNA occurs at rate  $k_p$ . Protein molecules  
466 are assumed to be stable (except for  $A$  in the oscillator circuit). Cell volume is growing  
467 exponentially at a fixed rate between  $V_{birth}$  and  $V_{div} = 2V_{birth}$ , then cell division is triggered  
468 (for the case including cell size control and variability see below). At cell division, molecules  
469 are randomly split between daughter cells and the volume is halved. In simulations, only

470 one of the daughter cell is considered for further simulation (hence mimicking the ‘mother  
471 machine’ microfluidic experiments for a symmetrically dividing cell (Wang *et al*, 2010).  
472 Throughout, noise is quantified by using coefficient of variability (CV), which is defined as  
473 standard deviation divided by the mean.

#### 474 **Reference gene expression parameters**

475 Realistic (Taniguchi *et al*, 2010) parameters for *E. coli* gene expression have been used  
476 ( $k_m = 0.28 \text{ min}^{-1}$ ,  $\gamma_m = 0.14 \text{ min}^{-1}$ ,  $k_p = 0.94 \text{ min}^{-1}$ ,  $\mu = 2$  doublings/hr). This corre-  
477 sponds to a mRNA half-life of 5 min, an average mRNA number at birth of 1 molecule  
478 and an average protein number at birth of 50 molecules.

#### 479 **Realistic modelling of cellular growth rate and cell size variability across** 480 **growth conditions with noisy linear maps**

481 We use *noisy linear maps* (Tanouchi *et al*, 2015) with parameters inferred from mother  
482 machine data in different growth conditions (Taheri-Araghi *et al*, 2015). See Supplemental  
483 Figure 1 for model description.  $a$  and  $b$  are estimated by linear regression of  $V_{div}$  vs  $V_{birth}$   
484 (the data contains around 100K cell cycles per condition).  $\sigma_1$  is by definition related to  
485 the residual of this regression.  $\sigma_2$  is estimated from the variance of  $\frac{V_{div}}{V_{birth}^{next}}$  where  $V_{birth}^{next}$  is  
486 the birth size recorded just after the division at  $V_{div}$ .

#### 487 **Modelling $Q$ expression by transcriptional or translational adjustment**

488 For a stable protein, it is possible to derive an analytical expression for the average number  
489 of protein molecules at birth:  $\langle P \rangle_{birth} = \frac{k_m k_p}{\gamma_m \mu} \left( 1 - \frac{\mu}{\gamma_m} \frac{1 - e^{-\gamma_m/\mu}}{2 - e^{-\gamma_m/\mu}} \right)$ .

490 This expression was used to compute the transcription or translation rate achieving a given

491 average protein concentration (Figure 3 and 4). In the case of active protein degradation (as  
492 for  $A$  for the oscillator circuit studied in Figure 5), we used simulations and the MATLAB  
493 scalar optimization function *fminsearch* to compute the transcriptional or translational  
494 rate adjustment enabling to maintain a constant average concentration at birth.

## 495 **Modelling $P$ expression**

496 For Figure 4, we have used division rate dependencies of gene expression parameters from  
497 (Klumpp *et al*, 2009) as illustrated in (Supplemental Figure 5). The dependencies were  
498 used as a relative scaling with respect to the reference gene expression parameters at 2  
499 doublings per hour. For modelling  $P$  expression in the oscillator circuit (Figure 5), for  
500 simplicity we simply used the effective transcription rate division rate dependency (the  
501 cell size dependency being given by the noisy linear maps) as change in translation rate  
502 per mRNA or mRNA degradation rate are small.

## 503 **Oscillator circuit**

504 The model structure and parameterization is adapted from (Vilar *et al*, 2002). The  $A$   
505 protein can transcriptionally activate its own expression as well as the expression of another  
506 protein  $R$  by promoter binding.  $A$  is short-lived while  $R$  is stable.  $A$  and  $R$  can form  
507 a complex. The same model reactions were used, but we also explicitly model growth  
508 and division (including random partitioning of free  $A$  and free  $R$ , but we do not model  
509 gene replication and consider a single copy of each promoter which is always inherited by  
510 daughter cells). The volume dependency of bi-molecular reactions is also accounted for.  
511 As reference parameters (i.e. corresponding to an intermediate *E. coli* division rate of 2  
512 doublings per hour, at which optimal circuit behavior should be obtained), we used the  
513 same parameters as Vilar and colleagues, except that the  $R$  degradation rate was set to

514 0 (the original value, corresponding to a  $\sim 200$  min half-life, was accounting for dilution  
515 only), the active degradation rate of  $A$  was scaled up to maintain a constant ratio with the  
516 division rate, the  $R$  translation rate was scaled up by the same factor, and all transcription  
517 rates were scaled by this factor ( $\sim 7$ ).

518 The resulting values are:

| Name         | Value              | Unit                 |
|--------------|--------------------|----------------------|
| $k_{on}^A$   | 0.0167             | $min^{-1}\mu m^{-3}$ |
| $k_{off}^A$  | 0.0833             | $min^{-1}$           |
| $k_m^{A,0}$  | 5.77               | $min^{-1}$           |
| $k_m^A$      | $10 * k_m^{A,0}$   | $min^{-1}$           |
| $\gamma_m^A$ | 0.167              | $min^{-1}$           |
| $k_p^A$      | 0.833              | $min^{-1}$           |
| $\gamma_P^A$ | 0.115              | $min^{-1}$           |
| $k_{on}^R$   | 0.0167             | $min^{-1}\mu m^{-3}$ |
| $k_{off}^R$  | 1.67               | $min^{-1}$           |
| $k_m^{R,0}$  | 0.00115            | $min^{-1}$           |
| $k_m^R$      | $5000 * k_m^{R,0}$ | $min^{-1}$           |
| $\gamma_m^R$ | 0.0083             | $min^{-1}$           |
| $k_p^R$      | 0.577              | $min^{-1}$           |
| $k_c$        | 0.033              | $min^{-1}\mu m^{-3}$ |

519 To compute the period and amplitude of oscillations in free  $R$  concentration, we used  
520 the MATLAB function *findpeaks* on very long (200K minutes) mother machine traces,  
521 requiring a minimum peak amplitude of 25% of the maximum value in the trace. We  
522 verified visually the behavior of the peak detection algorithm for each simulation.

## 523 Toggle switch circuit

524 The model structure and parameters are completely symmetric for the two proteins  
525 repressing each other. There is no cooperativity in the repression, as it is not required to  
526 obtain stochastic switching, consistently with (Lipshtat *et al*, 2006). As for the oscillator  
527 circuit, the volume dependency of bi-molecular reactions (only promoter binding here) was  
528 accounted for. We assumed that transcription is completely blocked when the promoters  
529 are bound, and that the promoter binding and unbinding rates are independent of the  
530 division rate.

531 The reference parameter values are:

| Name         | Value | Unit                 |
|--------------|-------|----------------------|
| $k_b$        | 1     | $min^{-1}\mu m^{-3}$ |
| $k_u$        | 0.25  | $min^{-1}$           |
| $k_m$        | 0.28  | $min^{-1}$           |
| $\gamma_m^A$ | 0.14  | $min^{-1}$           |
| $k_p$        | 0.94  | $min^{-1}$           |

532 Detection of bistability (always the case for simulations shown in Figure 5), threshold  
533 identification and computation of switching rates were performed as follows. A very long  
534 (500 thousands hours of biological time) single-lineage trace (one output every 15 minutes)  
535 of the free  $A$  concentration is obtained by simulation. This trace is then discretized into  
536 50 equal size bins from zero to the maximal value of the trace. The following algorithm  
537 is then applied on this discretized distribution: (1) identify the highest mode (i.e. the  
538 most populated bin); (2) iteratively identify next highest mode and ask whether they  
539 are corresponding to a neighbor bin of the highest mode (then it is not the second mode  
540 of a bimodal distribution) OR if there exists populated, lower height bins in-between

541 (indicative of bimodality); (3) in the latter case, to avoid incorrect detection of bimodality  
542 because of finite sampling of the distribution, the secondary mode is required to be more  
543 than 5% of what an uniform distribution would give.

## 544 Growth bistability caused by expression of a toxic protein

545 As previously, stochastic gene expression of a protein is simulated in growing and dividing  
546 cells. However, the protein is a toxin inhibiting cell growth: the instantaneous growth  
547 rate of the cell  $\mu_{cell}$  is a decreasing Hill function of the toxin concentration (hence it is  
548 not anymore constant during the cell cycle). Also, the impact of growth conditions is not  
549 modeled anymore with condition-specific noisy linear maps, as they are not adapted to  
550 situations with very heterogeneous growth rates between cells in a given condition. We  
551 rather use a parameter  $\mu_{max}$  representing the toxin-free cellular growth rate. For simplicity,  
552 to model cell division size and its variability we use a single noisy linear map across growth  
553 conditions. Finally, to represent the dependency of gene expression with the cell growth  
554 rate, we assume that the toxin transcription rate is a linear function of  $\mu_{cell}$ . The reference  
555 parameter values are:

| Name         | Value | Unit                    |
|--------------|-------|-------------------------|
| $\mu_{max}$  | 2     | doublings/hr            |
| $km_0$       | 0.28  | $min^{-1}$              |
| $km_{slope}$ | 0     | $min^{-1}/doublings/hr$ |
| $\gamma_m$   | 0.14  | $min^{-1}$              |
| $k_p$        | 0.94  | $min^{-1}$              |
| $\gamma_p$   | 0.001 | $min^{-1}$              |
| $n$          | 2     | dimensionless           |
| $T^*$        | 140   | $\#/\mu m^3$            |

| Name             | Value | Unit          |
|------------------|-------|---------------|
| $a_{lnm}$        | 1     | dimensionless |
| $b_{lnm}$        | 1     | $\mu m^3$     |
| $\sigma_1^{lnm}$ | 0.2   | $\mu m^3$     |
| $\sigma_2^{lnm}$ | 0.05  | dimensionless |

556 Note that because  $km_{slope} = 0$ , the positive feedback toxin  $\rightarrow$  growth slow down  $\rightarrow$  more  
557 toxin is only mediated by a change of dilution (as in (Rocco *et al*, 2013)). Also note  
558 that it is necessary to assume that protein degradation is non-zero to allow bistability, as  
559 otherwise exit of the slow state is impossible.

560 For Figure 7-C, for each parameter set, the existence of bistability, threshold identification  
561 and switching rates computation for the instantaneous cell growth rate  $\mu_{cell}$  were performed  
562 as for the toggle switch circuit analysis (except that simulation duration for each single-  
563 lineage trace was 60 thousands hours of biological time, with one output every 10 minutes,  
564 and the number of bins used was 20).

565 Grey indicates parameter sets for which the lineage simulation of 60 thousands hours  
566 ( $\sim 120$  thousands generations) either did not lead to a bimodal distribution of  $\mu_{cell}$ , or did  
567 lead to such bimodal distribution, but with less than 10 switches fast  $\rightarrow$  slow  $\rightarrow$  fast,  
568 preventing an accurate estimate of switching rates in reasonable computational time.

## 569 **Simulation algorithm**

570 We describe here the general simulation algorithm used for all models. Between fixed  
571 timesteps (6 seconds), cell volume is considered constant, and the Gillespie algorithm is used  
572 to simulate stochastic molecular reactions (more sophisticated simulation methods exist  
573 (Lu *et al*, 2004; Shahrezaei *et al*, 2008), but this one is simple to implement and accurate



574 as long as the timestep is small enough). Then, the cell volume is updated according to the  
575 instantaneous exponential growth rate, it is checked whether cell division should occur, and  
576 if so, cell division and molecules partitioning is realized. The code used for all simulations  
577 is available on GitHub: <https://github.com/ImperialCollegeLondon/coli-noise-and-growth>.

## 578 **References**

- 579 Antunes D & Singh A (2014) Quantifying gene expression variability arising from random-  
580 ness in cell division times. *Journal of Mathematical Biology*
- 581 Basan M, Hui S, Okano H, Zhang Z, Shen Y, Williamson JR & Hwa T (2015) Overflow  
582 metabolism in *Escherichia coli* results from efficient proteome allocation. *Nature* **528**:  
583 99–104
- 584 Bertaux F, Von Kügelgen J, Marguerat S & Shahrezaei V (2016) A unified coarse-grained  
585 theory of bacterial physiology explains the relationship between cell size, growth rate and  
586 proteome composition under various growth limitations. *bioRxiv*
- 587 Berthoumieux S, Jong H de, Baptist G, Pinel C, Ranquet C, Ropers D & Geiselmann J  
588 (2013) Shared control of gene expression in bacteria by transcription factors and global  
589 physiology of the cell. *Molecular Systems Biology* **9**: 634–634
- 590 Bierbaum V & Klumpp S (2015) Impact of the cell division cycle on gene circuits. *Physical*  
591 *biology* **12**: 066003
- 592 Borkowski O, Goelzer A, Schaffer M, Calabre M, Mäder U, Aymerich S, Jules M & Fromion  
593 V (2016) Translation elicits a growth rate-dependent, genome-wide, differential protein  
594 production in *Bacillus subtilis*. *Molecular Systems Biology* **12**: 870–14
- 595 Ceroni F, Algar R, Stan G-B & Ellis T (2015) Quantifying cellular capacity identifies gene

- 596 expression designs with reduced burden. *Nature methods* **12**: 415–418
- 597 Cookson NA, Cookson SW, Tsimring LS & Hasty J (2010) Cell cycle-dependent variations  
598 in protein concentration. *Nucleic acids research* **38**: 2676–2681
- 599 Dai X, Zhu M, Warren M, Balakrishnan R, Patsalo V, Okano H, Williamson JR, Fredrick  
600 K, Wang Y-P & Hwa T (2016) Reduction of translating ribosomes enables *Escherichia*  
601 *coli* to maintain elongation rates during slow growth. *Nature Microbiology* **2**: 16231
- 602 Elowitz MB, Levine AJ, Siggia ED & Swain PS (2002) Stochastic gene expression in a  
603 single cell. *Science (New York, N.Y.)* **297**: 1183–1186
- 604 García-Martínez J, Delgado-Ramos L, Ayala G, Pelechano V, Medina DA, Carrasco F,  
605 González R, Andrés-León E, Steinmetz L, Warringer J, Chávez S & Pérez-Ortín JE  
606 (2016) The cellular growth rate controls overall mRNA turnover, and modulates either  
607 transcription or degradation rates of particular gene regulons. *Nucleic acids research* **44**:  
608 3643–3658
- 609 Gardner TS, Cantor CR & Collins JJ (2000) Construction of a genetic toggle switch in  
610 *Escherichia coli*. *Nature* **403**: 339–342
- 611 Gerosa L, Kochanowski K, Heinemann M & Sauer U (2013) Dissecting specific and global  
612 transcriptional regulation of bacterial gene expression. *Molecular Systems Biology* **9**:  
613 658–658
- 614 Goelzer A & Fromion V (2017) Resource allocation in living organisms. *Biochemical*  
615 *Society transactions*
- 616 Gonze D (2013) Modeling the effect of cell division on genetic oscillators. *Journal of*  
617 *Theoretical Biology* **325**: 22–33
- 618 Görke B & Stülke J (2008) Carbon catabolite repression in bacteria: many ways to make

- 619 the most out of nutrients. *Nature reviews. Microbiology* **6**: 613–624
- 620 Guantes R & Poyatos JF (2006) Dynamical principles of two-component genetic oscillators.  
621 *PLoS computational biology* **2**: e30
- 622 Huh D & Paulsson J (2011) Random partitioning of molecules at cell division. *Proceedings*  
623 *of the National Academy of Sciences of the United States of America* **108**: 15004–15009
- 624 Hui S, Silverman JM, Chen SS, Erickson DW, Basan M, Wang J, Hwa T & Williamson  
625 JR (2015) Quantitative proteomic analysis reveals a simple strategy of global resource  
626 allocation in bacteria. *Molecular Systems Biology* **11**: e784
- 627 Johnston IG, Gaal B, Neves RP das, Enver T, Iborra FJ & Jones NS (2012) Mitochondrial  
628 variability as a source of extrinsic cellular noise. *PLoS computational biology* **8**: e1002416
- 629 Jun S & Taheri-Araghi S (2015) Cell-size maintenance: universal strategy revealed. *Trends*  
630 *in Microbiology* **23**: 4–6
- 631 Kempe H, Schwabe A, Crémazy F, Verschure PJ & Bruggeman FJ (2015) The volumes  
632 and transcript counts of single cells reveal concentration homeostasis and capture biological  
633 noise. *Molecular biology of the cell* **26**: 797–804
- 634 Keren L, Dijk D van, Weingarten-Gabbay S, Davidi D, Jona G, Weinberger A, Milo R  
635 & Segal E (2015) Noise in gene expression is coupled to growth rate. *Genome research*:  
636 gr.191635.115
- 637 Keren L, Zackay O, Lotan-Pompan M, Barenholz U, Dekel E, Sasson V, Aidelberg G,  
638 Bren A, Zeevi D, Weinberger A, Alon U, Milo R & Segal E (2013) Promoters maintain  
639 their relative activity levels under different growth conditions. *Molecular Systems Biology*  
640 **9**: 701–701
- 641 Kiviet DJ, Nghe P, Walker N, Boulineau S, Sunderlikova V & Tans SJ (2014) Stochasticity

- 642 of metabolism and growth at the single-cell level. *Nature* **514**: 376–379
- 643 Klumpp S, Scott M, Pedersen S & Hwa T (2013) Molecular crowding limits translation  
644 and cell growth. *Proceedings of the National Academy of Sciences* **110**: 16754–16759
- 645 Klumpp S, Zhang Z & Hwa T (2009) Growth Rate-Dependent Global Effects on Gene  
646 Expression in Bacteria. *Cell* **139**: 1366–1375
- 647 Kut C, Golkhou V & Bader JS (2009) Analytical approximations for the amplitude and  
648 period of a relaxation oscillator. *BMC systems biology* **3**: 6
- 649 Li G-W, Burkhardt D, Gross C & Weissman JS (2014) Quantifying absolute protein  
650 synthesis rates reveals principles underlying allocation of cellular resources. *Cell* **157**:  
651 624–635
- 652 Lipshtat A, Loinger A, Balaban NQ & Biham O (2006) Genetic toggle switch without  
653 cooperative binding. *Physical review letters* **96**: 188101
- 654 Lloyd-Price J, Tran H & Ribeiro AS (2014) Dynamics of small genetic circuits subject to  
655 stochastic partitioning in cell division. *Journal of Theoretical Biology* **356**: 11–19
- 656 Lu T, Volfson D, Tsimring L & Hasty J (2004) Cellular growth and division in the Gillespie  
657 algorithm. *Systems biology*
- 658 Luo R, Ye L, Tao C & Wang K (2013) Simulation of E. coli Gene Regulation including  
659 Overlapping Cell Cycles, Growth, Division, Time Delays and Noise. *PLoS ONE* **8**:  
660 e62380–10
- 661 Modi S, Vargas-Garcia CA, Ghusinga KR & Singh A (2017) Analysis of Noise Mechanisms  
662 in Cell-Size Control. *Biophysical journal* **112**: 2408–2418
- 663 Molenaar D, Berlo R van, Ridder D de & Teusink B (2009) Shifts in growth strategies

- 664 reflect tradeoffs in cellular economics. *Molecular Systems Biology* **5**: 323
- 665 Osella M & Lagomarsino MC (2013) Growth-rate-dependent dynamics of a bacterial  
666 genetic oscillator. *Physical review. E, Statistical, nonlinear, and soft matter physics* **87**:  
667 012726
- 668 Padovan-Merhar O, Nair GP, Biaesch AG, Mayer A, Scarfone S, Foley SW, Wu AR, Church-  
669 man LS, Singh A & Raj A (2015) Single Mammalian Cells Compensate for Differences in  
670 Cellular Volume and DNA Copy Number through Independent Global Transcriptional  
671 Mechanisms. *Molecular Cell* **58**: 339–352
- 672 Paijmans J, Bosman M, Wolde PR ten & Lubensky DK (2016) Discrete gene replication  
673 events drive coupling between the cell cycle and circadian clocks. *Proceedings of the*  
674 *National Academy of Sciences* **113**: 4063–4068
- 675 Peterson JR, Cole JA, Fei J, Ha T & Luthey-Schulten ZA (2015) Effects of DNA replication  
676 on mRNA noise. *Proceedings of the National Academy of Sciences of the United States of*  
677 *America* **112**: 15886–15891
- 678 Rocco A, Kierzek AM & McFadden J (2013) Slow protein fluctuations explain the emergence  
679 of growth phenotypes and persistence in clonal bacterial populations. *PLoS ONE* **8**: e54272
- 680 Schaechter M, Maaloe O & Kjeldgaard NO (1958) Dependency on medium and temperature  
681 of cell size and chemical composition during balanced grown of *Salmonella typhimurium*.  
682 *Journal of general microbiology* **19**: 592–606
- 683 Schwabe A & Bruggeman FJ (2014) Contributions of Cell Growth and Biochemical  
684 Reactions to Nongenetic Variability of Cells. *Biophysical journal* **107**: 301–313
- 685 Scott M, Gunderson CW, Mateescu EM, Zhang Z & Hwa T (2010) Interdependence of cell  
686 growth and gene expression: origins and consequences. *Science (New York, N.Y.)* **330**:

687 1099–1102

688 Scott M, Klumpp S, Mateescu EM & Hwa T (2014) Emergence of robust growth laws  
689 from optimal regulation of ribosome synthesis. *Molecular Systems Biology* **10**: 747

690 Shahrezaei V & Marguerat S (2015) Connecting growth with gene expression: of noise  
691 and numbers. *Current opinion in microbiology* **25**: 127–135

692 Shahrezaei V & Swain PS (2008) Analytical distributions for stochastic gene expression.  
693 *Proceedings of the National Academy of Sciences* **105**: 17256–17261

694 Shahrezaei V, Ollivier JF & Swain PS (2008) Colored extrinsic fluctuations and stochastic  
695 gene expression. *Molecular Systems Biology* **4**: 196

696 Soltani M, Vargas-Garcia CA, Antunes D & Singh A (2016) Intercellular Variability  
697 in Protein Levels from Stochastic Expression and Noisy Cell Cycle Processes. *PLoS*  
698 *computational biology* **12**: e1004972

699 Swain PS, Elowitz MB & Siggia ED (2002) Intrinsic and extrinsic contributions to  
700 stochasticity in gene expression. *Proceedings of the National Academy of Sciences of the*  
701 *United States of America* **99**: 12795–12800

702 Taheri-Araghi S, Bradde S, Sauls JT, Hill NS, Levin PA, Paulsson J, Vergassola M & Jun  
703 S (2015) Cell-size control and homeostasis in bacteria. *Current biology : CB* **25**: 385–391

704 Tan C, Marguet P & You L (2009) Emergent bistability by a growth-modulating positive  
705 feedback circuit. *Nature Chemical Biology*

706 Taniguchi Y, Choi PJ, Li G-W, Chen H, Babu M, Hearn J, Emili A & Xie XS (2010)  
707 Quantifying *E. coli* proteome and transcriptome with single-molecule sensitivity in single  
708 cells. *Science (New York, N. Y.)* **329**: 533–538

709 Tanouchi Y, Pai A, Park H, Huang S, Stamatov R, Buchler NE & You L (2015) A noisy

- 710 linear map underlies oscillations in cell size and gene expression in bacteria. *Nature*  
711 *Publishing Group* **523**: 357–360
- 712 Turner JJ, Ewald JC & Skotheim JM (2012) Cell size control in yeast. *Current biology* :  
713 *CB* **22**: R350–9
- 714 Vilar JMG, Kueh HY, Barkai N & Leibler S (2002) Mechanisms of noise-resistance in  
715 genetic oscillators. *Proceedings of the National Academy of Sciences of the United States*  
716 *of America* **99**: 5988–5992
- 717 Walker N, Nghe P & Tans SJ (2016) Generation and filtering of gene expression noise by  
718 the bacterial cell cycle. *BMC Biology* **14**: 11
- 719 Wallden M, Fange D, Lundius EG, Baltekin Ö & Elf J (2016) The Synchronization of  
720 Replication and Division Cycles in Individual E. coli Cells. *Cell* **166**: 729–739
- 721 Wang P, Robert L, Pelletier J, Dang WL, Taddei F, Wright A & Jun S (2010) Robust  
722 growth of Escherichia coli. *Current biology* : *CB* **20**: 1099–1103
- 723 Zopf CJ, Quinn K, Zeidman J & Maheshri N (2013) Cell-cycle dependence of transcription  
724 dominates noise in gene expression. **9**: e1003161